Microchim Acta
DOI 10.1007/s00604-015-1518-4

ORIGINAL PAPER

Microsphere-based immunoassay integrated with a microfluidic network to perform logic operations

Pooja Sabhachandani[1] · **Noa Cohen**[1] · **Saheli Sarkar**[1] · **Tania Konry**[1]

Received: 8 March 2015 / Accepted: 4 May 2015

Abstract Lab on a chip (LOC) intelligent diagnostics can be described by molecular logic-based circuits. We report on the development of an LOC approach with logic capability for screening combinations of antigen and antibody in the same sample. A microsphere-based immunoassay was integrated with a microfluidic network device to perform the logic operations AND and INHIBIT. Using the clinically relevant biomarkers TNF-α cytokine and anti-TNF-α antibody, we obtained a fluorescent output in the presence of both inputs. This results in an AND operation, while the presence of only one specific input results in a different fluorescent signal, thereby indicating the INHIBIT operation. This approach demonstrates the effective use of molecular logic computation for developing portable, point-of-care technologies for diagnostic purposes due to fast detection times, minimal reagent consumption and low costs. This model system may be further expanded to screening of multiple disease markers, combinatorial logic applications, and developing "smart" sensors and therapeutic technologies.

Keywords Molecular logic gates · Boolean logic operations · Microfluidics · TNF -α · Anti-TNF-α · Immunoassay · Point-of-care diagnostics

Pooja Sabhachandani and Noa Cohen contributed equally to this work.

✉ Tania Konry
t.konry@neu.edu

[1] Department of Pharmaceutical Sciences, School of Pharmacy, Bouve' College of Health Sciences, Northeastern University, 140 The Fenway, Boston, MA 02115, USA

Introduction

Microfluidic technologies have been widely used to miniaturize existing biochemical assays and develop highly sophisticated Micro-Total Analysis Systems (μTAS) that allow novel insights in physical, chemical and biological sciences [1, 2]. Lab-on-a-chip (LOC) systems utilize pico- to nano-liters of fluids under precisely controlled conditions to synthesize complex chemical compounds [3], perform high throughput screening and sorting [4–8] and assess various biological processes in living cells and tissues [9–12]. Microfluidic LOCs not only have the potential to surpass conventional laboratory equipment in complexity, sensitivity and reduced duration of experiments [13–16], but also provide opportunities for innovative applications, such as molecular logic gates, that do not have traditional analogs.

The concept of data storage and processing by molecular-level computation is fast gaining popularity due to the saturation of physical limits of electronic circuitry. Molecular logic gates have been designed to perform classic Boolean operations using fluorescent small molecules, DNA oligonucleotides, reversible proteins, fluorophores, chromophores and nanoparticles [17, 18]. Features such as miniature scale, precise control over synthesis and operation and fast response times make molecular logic gates feasible in biomedical informatics. The combination of chemical inputs based on pH, metal ions and anions and fluorescence outputs have been utilized to develop logic gates such as AND, OR, XOR, NAND, NOR and INHIBIT [19, 20] Rapid progress has been made in this field in the past decade, with the development of complex logical arrays [21], sequential communication [22] and logic evaluation on live cell surfaces [23].

Published online: 14 May 2015

A programmable molecular logic-based network was demonstrated in microfluidic systems by exploiting pH changes and Cu^{2+} ions as inputs [24]. This valve-based device was able to perform XOR and INHIBIT functions as well as combinatorial half adder operations in solution phase. Droplet microfluidic platforms were applied to perform logic operations based on nonlinear change in hydrodynamic resistance inside droplet-containing channels [25] and passive pumping technique relying on difference in pressure between surfaces with varying curvature [26]. Embedded electronic detectors and external circuit controlling signal processing were used to obtain all 16 logic gates in a droplet microfluidic device [27]. In a different approach, our group's previous work demonstrated the possibility of performing medical diagnostics using logic operations [28]. The presence of two biological species, protein and DNA, was realized as AND output while the presence of protein alone resulted in INHIBIT function. The output consisted of fluorescence signatures corresponding to the unique optical barcoding on antibody- functionalized microspheres integrated in microwells.

Herein, a multiplexed microsphere-based immunoassay was integrated into a microfluidic LOC device that performs simple logic operations by coupling multiple molecular recognition inputs to a fluorescence signal output. Microsphere-based immunoassays are currently used for rapid high throughput screening of disease markers and sero-diagnosis of microbial products [29, 30]. This approach was used in our recent work, demonstrating fast reaction kinetics and near real- time detection of a clinically relevant analyte, Tumor Necrosis Factor-α (TNF-α) cytokine and antibody [31]. This is attributable to the large surface to volume ratio of the functionalized microspheres, leading to reaction rates comparable with solution- phase kinetics. Furthermore, the developed microfluidic LOC demonstrated ultra-fast analyte detection as well as required minimal reagent and sample volumes, making it suitable for assaying rare and low-abundance clinical analytes.

In this study, we investigated AND and INHIBIT (NOTIF) logic gates that respond to the presence of both antigen and antibody in microsphere-based microfluidic device. We chose TNF-α as a model biomolecule as it has been implicated in various pathological conditions, including cancer and Alzheimer's disease [32]. Anti- TNF-α antibodies are considered highly effective in the treatment of various disorders [33]. Therefore, simultaneous detection of TNF-α and its administered inhibitors is pertinent in diseased states as well as in pharmacokinetic characterization of drug screening studies [34]. Our results suggest that this microfluidic immunoassay-based logic operation can be used for smart diagnosis of disease markers in a continuous, real-time format.

Experimental

Microfluidic device fabrication

The microfluidic device used for the experiments was fabricated with poly(dimethylsiloxane) (PDMS) as described below. Silicon wafers were spin coated with negative photo resist SU-8 2100 (MicroChem, Newton, MA, http://www.microchem.com/) to a thickness of 150 μm. The wafer was subsequently patterned by UV light exposure using a transparency photomask (CAD/Art Services, USA). PDMS (Sylgard 184, Dow Corning, MI, https://www.dowcorning.com/) and the crosslinker (Sylgard 184 curing agent) were mixed in a ratio of 10:1, deposited onto the patterned wafer, degassed and cured for 12 h at 65 °C. After curing, the PDMS was peeled off the wafers; individual devices were separated and bonded to a glass slide following treatment in an oxygen-plasma chamber. An individual device consisted of 3 inlets and 2 serpentine mixing regions. 1 mL syringes containing input reagents were connected to the device using Tygon Micro Bore PVC Tubing (dimensions: 0.010″ ID, 0.030″ OD 0.010″ Wall, Small Parts Inc, FL, USA, http://www.smallpartsinc.com/). The flow rate through the device was maintained at 1 $\mu L \cdot min^{-1}$ using syringe pumps (Harvard Apparatus, USA, https://www.harvardapparatus.com/webapp/wcs/stores/servlet/catalog_11051_10001_-1_HAI).

Conjugation of streptavidin microspheres to biotinylated TNF- α protein for anti- TNF- α antibody detection

The functionalized microspheres described below were used for the inputs (1,0), (0,0) and (1,1) for the INHIBIT logic gate experiments. A 50 μL aliquot of streptavidin-coated polystyrene microspheres (diameter 6.8 μm, 0.5 % *w/v*, Spherotech Inc., http://www.spherotech.com/) was diluted to a concentration of 0.25 $mg \cdot mL^{-1}$ in Phosphate Buffer Saline (PBS) with 0.005 % (*v/v*) Tween 20 (Sigma, USA, https://www.sigmaaldrich.com/united-states.html). 40 μg of biotinylated human TNF-α protein (Cat. No. TNA-H8211, ACRO Biosystem, http://www.acrobiosystems.com/) was added to 1 mg of microspheres, and the mixture was shaken at room temperature (RT) for 120 min. Unbound active sites were blocked with BlockAid (B-10710, Invitrogen, http://www.lifetechnologies.com/us/en/home/brands/invitrogen.html) for 60 min. Finally, the microspheres were washed with PBS and stored at 4 °C in 0.5 % (*w/v*) Bovine Serum Albumin (BSA) (Sigma, USA) in PBS.

The analyte for the experiments, mouse monoclonal antibody to human TNF-α (Cat. No. 10602-MM01, Sino

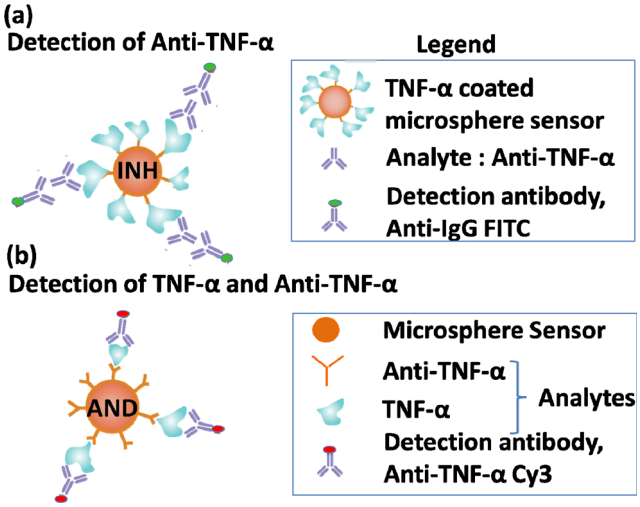

Fig. 1 Schematic illustration of the **a** Anti-TNF-α antibody and **b** Anti - TNF-α antibody - TNF-α protein microsphere sensors

Biological Inc., USA, http://www.sinobiological.com/), was diluted to a concentration of 500 ng·mL^{-1} in 1X PBS. The detection antibody, goat anti-mouse IgG-FITC (Cat. No. F 0257, Sigma, USA) was mixed with Pierce Immunostain Enhancer (Thermo Scientific, USA, http://www.thermoscientific.com/en/home.html) to obtain a final concentration of 13.8 μg·mL^{-1}.

Conjugation of protein G microspheres to anti-human TNF-α antibody for TNF-α detection

The conjugated microspheres described here were used for the inputs (0,1) and (1,1) for the AND logic gate experiments. A 200 μL (1 mg) aliquot of Protein G polystyrene microspheres (0.5 % *w/v*, Spherotech Inc.) was conjugated to anti-human/rat TNF-α (Thermo Scientific, USA, Cat. No. P300A) as discussed above with the following modifications: 200 μL of rabbit anti-human TNF-α was diluted with 100 μL of 0.5 % BSA/PBS (0.22 mg) and added to the microspheres for conjugation.

The analyte for the experiments, E. coli-derived recombinant rat TNF-α (Cat. No. AGM0213082, R&D Systems, USA, http://www.rndsystems.com/), was diluted to a concentration of 1000 ng·mL^{-1} in 1X PBS. The fluorescently labeled detection antibody (anti-mouse/rat-TNF-α eFluor® 660, eBioscience, USA, Cat. No. 50-7423, http://us.ebioscience.com/) was diluted to a final concentration of 13.8 μg·mL^{-1} using Pierce Immunostain Enhancer. For flow simulation of the particles in the device we used streptavidin fluoresbrite YG Microspheres (diameter 6.2 μm, 1.3 % *w/v*, Polysciences Inc., Cat. No. 24157, http://www.polysciences.com/) and streptavidin coated fluorescent Nile red particles (diameter 7.34 μm, 0.1 % *w/v*, Spherotech Inc., Cat. No. SVFP-6056-5).

Data and image analysis

All images were acquired with Zeiss Axio Observer.Z1 Microscope (Zeiss, Germany, http://www.zeiss.com/corporate/en_us/home.html) equipped with Hamamatsu digital camera C10600 Orca-R2 and ZEN pro 2012 software (blue edition). ImageJ was used for fluorescence analysis and image processing. A minimum of thirty microspheres was analyzed for each condition. For each sample, the selected microsphere area, integrated density and mean gray value were measured. The background fluorescence was measured as a randomly

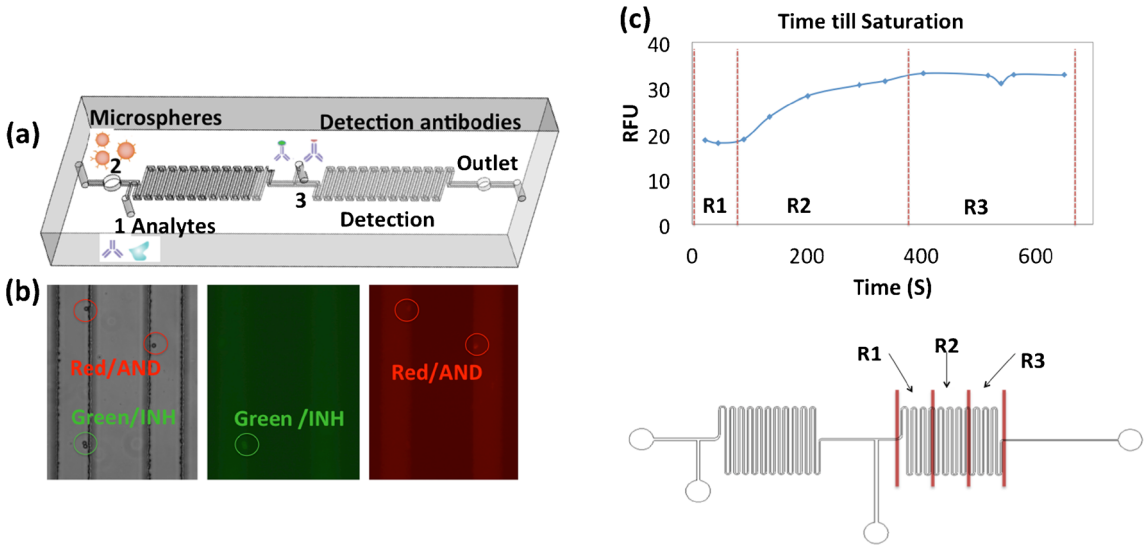

Fig. 2 **a** Schematic illustration of the LOC. **b** Detection of the analytes in the incubation channels; INH gate FITC green, AND gate eFluor® 660 Red. **c** Development of the fluorescence on the microsphere over the course of time in the device. *RFU* represents Relative Fluorescence Unit. R1, R2, R3 represent Regions 1, 2, and 3 respectively of the detection channels as indicated in the lower panel

(a)

Input 1 TNF-α	Input 2 Anti- TNF-α	Output AND gate	Output INH gate
1	0	0	0
1	1	1	0
0	1	0	1

(b)

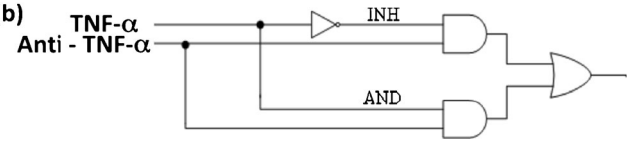

Fig. 3 **a** Truth table for logic gates and **b** AND and INHIBIT logic gates

selected area close to the microsphere region in the microfluidic channel. The average background intensity is subtracted from the microsphere fluorescence intensity and represented as Normalized Fluorescent Intensity (NFI). Microsoft Office Excel 2010 was used for statistical analysis of the data.

Results and discussion

Multiplex microsphere based assay for simultaneous protein and antibody detection

Herein we present a microsphere based multiplex assay for simultaneous protein and antibody detection in bio-samples (Fig. 1a and b). For anti- TNF-α antibody detection, avidinylated microspheres were conjugated off-chip to biotinylated human TNF-α protein via avidin-biotin bridge [31] as described in the Experimental Section. These microsphere-based sensors are capable of capturing the analyte, mouse monoclonal anti-human TNF-α antibody (Fig. 1a). Next, the detection antibody, FITC-labeled anti-mouse IgG, is introduced to label the previously captured anti- TNF-α protein. The fluorescent signal on the microsphere sensor, generated by the conjugation of the captured anti-TNF-α antibody with the fluorescently labeled detection antibody is demonstrated in Fig. 2b. For TNF-α and anti-TNF-α antibody simultaneous detection, protein-G microspheres were conjugated to anti–TNF-α antibodies as described in the Experimental Section. Next, the generated microsphere-based sensors were introduced to the analyte, TNF-α. The interaction of the two components resulted in the binding of TNF-α by previously captured anti-TNF-α antibody on microsphere surface in. Lastly, the detection antibody, eFluor® 660 red fluorescence -labeled anti - rat TNF-α antibody, was introduced so as to provide fluorescent detection.

Integration of multiplex microsphere based assay with microfluidics device

To make the overall platform programmable, the above-described microsphere sensors were incorporated into the design of the microfluidic system. The detection of the analytes in the microfluidic system is monitored by fluorescence signal generated on the surface of microsphere sensors that performs the computation in a real time format. Briefly, the device consists of three inlets and two serpentine mixing regions. Figure 2 schematically illustrates a flow-through microsphere-based immunoassay in microfluidic device. First, a solution containing the analytes (such as the antigen, TNF-α, and the antibody, anti- TNF-α) is introduced via inlet 1. A suspension of microsphere sensors functionalized with the capture molecule against the target analyte is added into inlet 2. As the microsphere sensors and analytes flow through the serpentine channel, they are intermixed due to the curved channel geometry, thus allowing rapid analyte capture on the surface of the microsphere sensors. Secondary antibodies against the analytes, conjugated with specific fluorophores, are then introduced through inlet 3 into the flow stream just before the second serpentine mixing structure (Fig. 2). The mixing generated

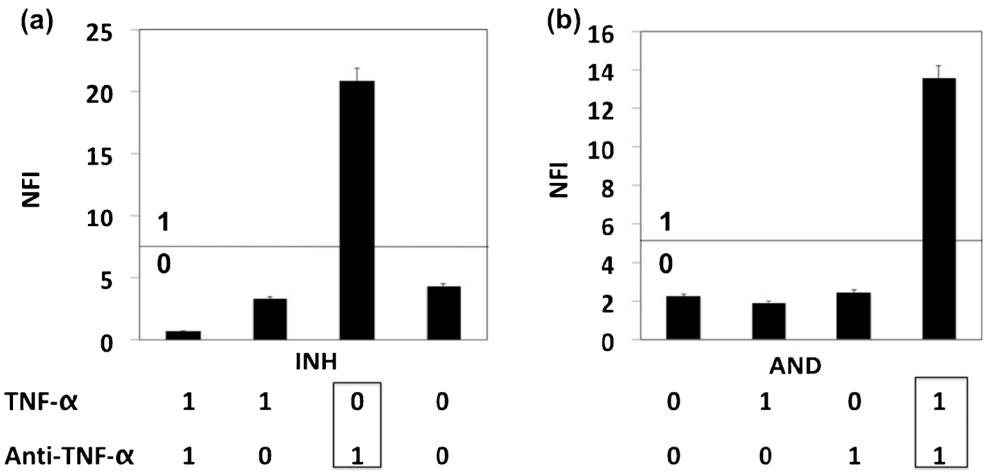

Fig. 4 Output averaged fluorescence intensities in the absence (*0*) or in the presence (*1*) of analyte (TNF-α=1000 ng·mL^{-1}, Anti- TNF-α=500 ng·mL^{-1}). *NFI* represents Normalized Fluorescence Intensityy

within the serpentine structure of microfluidic device results in the formation of triple layered complex consisting of detection antibody-antigen-reporter antibody on the surface of the sensors. The high surface-to-volume ratio of the microsphere, as well as the fast mixing and binding kinetics, reduces the equilibration time to seconds, thereby enabling detection during continuous flow-through [31]. Sufficient accumulation of the reporter antibody leads to localized fluorescence on the microsphere, which is easily distinguishable from the much lower background intensity.

We were able to follow the fluorescent detection signal development over the course of time in the detection region of the device. As shown in Fig. 2b, the fluorescent detection (RFU, relative fluorescent units) for a concentration of 500 $ng \cdot mL^{-1}$ could be measured after 22 s while reaching saturation after 400 s (Fig. 2c). Thus we were able to enhance the reaction rate and allow near real time dynamic in flow detection of the analyte in the passive micro mixed microchannels of the device [31].

Programmable microfluidics via microsphere based sensors

Herein, we demonstrate both AND and INHIBIT (NOTIF) logic gates that respond to the presence of antibody and both antigen and antibody in a sample. It is thus possible to use the resulting logic network for detection of TNF-α and its inhibitor, anti-TNF-α antibody, via microsphere-based immunoassays using a Boolean operator truth table (Fig. 3a). A schematic illustration of the TNF-α protein and anti -TNF-α antibody in microsphere sensors is shown in Fig. 1a and b. The sensor circuitry described here incorporates the AND and INHIBIT logic gate functionalities (Fig. 3).

The action of the INHIBIT gate can be described as a combination of the AND and NOT logic functions. Its action is such that an active input signal has a negative effect, which results in the inhibition of the signal. In our system, this corroborates the presence or the absence of antibody in the sample. The sole presence of anti-TNF-α antibody in the sample (input (0,1)) results in the emission of green fluorescence (output 1) as a consequence of the gate being switched on (Figs. 3 and 4a). Consequently, the absence of anti-TNF-α antibody in the sample (inputs (0,0) and (1,0)), produces no fluorescent emission of any kind i.e., the output signal is 0. The positive signal threshold (1) in Fig. 4 indicates the detection limit of the immunosensor. This is defined as the amount (or concentration) of the analyte that results in a response significantly higher (three standard deviations) than the background intensity value. Any signal below this threshold is considered as 'no response' (0).

Figure 4b represents the AND logic gate, which shows a positive output signal only when both the input signals are present. In our system, the two input signals were the presence of both, TNF-α protein and anti- TNF-α antibody. The experiments were performed with both the biological entities present in the same sample (input (1,1)), to test the multiplexing capabilities of the LOC device (Fig. 4b). A positive signal for the AND gate was observed by the means of eFluor® 660 red fluorescence emission. When one of the biological entities, either protein or the antibody were absent, or when both were absent (inputs (1,0), (0,1), (0,0)), the output signal obtained was negative i.e., no red fluorescence was observed. Thus in our system, the absence of one input analyte has the capability to disable the system in its entirety, regardless of the presence of other input signals.

Conclusion

In summary, we have demonstrated a microfluidic platform for the ultra fast and simultaneous detection of protein antigens and antibodies using molecular logic gates. The fluorescence outputs for a combination of input signals were interpreted using the truth table for the AND and INHIBIT logic gates, which verified the feasibility for the use of molecular logic for medical diagnostics. This technique could potentially be used for the screening of various medical conditions involving various combinations of diagnostic markers to provide fast and accurate results in a short period of time.

Acknowledgments We thank Ms. Vinny Motwani and Mr. Micah Amdur-Clark for their assistance in the preparation of Microfluidic devices for the experiments.

References

1. Dittrich PS, Manz A (2006) Lab-on-a-chip: microfluidics in drug discovery. Nat Rev Drug Discov 5:210–218. doi:10.1038/nrd1985
2. Kovarik ML, Ornoff DM, Melvin AT, Dobes NC, Wang Y, Dickinson AJ, Gach PC, Shah PK (2013) Allbritton NL (2013) Micro total analysis systems: fundamental advances and applications in the laboratory, clinic, and field. Anal Chem 85(2):451–472. doi:10.1021/ac3031543
3. Elvira KS, Casadevall i Solvas X, Wootton RC, deMello AJ (2013) The past, present and potential for microfluidic reactor technology in chemical synthesis. Nat Chem 5:905–915. doi:10.1038/nchem.1753
4. King KR, Wang S, Irimia D, Jayaraman A, Toner M, Yarmush ML (2007) A high-throughput microfluidic real-time gene expression living cell array. Lab Chip 7:77–85. doi:10.1039/B612516F
5. Brouzes E, Medkova M, Savenelli N, Marran D, Twardowski M, Hutchison JB, Rothberg JM, Link DR, Perrimon N, Samuels ML (2009) Droplet microfluidic technology for single-cell high-throughput screening. Proc Natl Acad Sci U S A 106:14195–14200. doi:10.1073/pnas.0903542106
6. Eastburn DJ, Sciambi A, Abate AR (2013) Ultrahigh-throughput Mammalian single-cell reverse-transcriptase polymerase chain reaction in microfluidic drops. Anal Chem 85:8016–8021. doi:10.1021/ac402057q

7. Warkiani ME, Khoo BL, Tan DS, Bhagat AA, Lim WT, Yap YS, Lee SC, Soo RA, Han J, Lim CT (2014) An ultra-high-throughput spiral microfluidic biochip for the enrichment of circulating tumor cells. Analyst 139:3245–3255. doi:10.1039/c4an00355a
8. Najah M, Calbrix R, Mahendra-Wijaya IP, Beneyton T, Griffiths AD, Drevelle A (2014) Droplet-based microfluidics platform for ultra-high-throughput bioprospecting of cellulolytic microorganisms. Chem Biol 21(12):1722–1732. doi:10.1016/j.chembiol.2014.10.020
9. Mao X, Huang TJ (2012) Exploiting mechanical biomarkers in microfluidics. Lab Chip 12:4006–4009. doi:10.1039/C2LC90100E
10. Golberg A, Linshiz G, Kravets I, Stawski N, Hillson NJ, Yarmush ML, Marks RS, Konry T (2014) Cloud-enabled microscopy and droplet microfluidic platform for specific detection of Escherichia coli in water. PLoS ONE 9(1):e86341. doi:10.1371/journal.pone.0086341
11. Hughes AJ, Herr AE (2012) Microfluidic western blotting. Proc Natl Acad Sci U S A 109:21450–21455. doi:10.1073/pnas.1207754110
12. Marcus JS, Anderson WF, Quake SR (2006) Microfluidic single-cell mRNA isolation and analysis. Anal Chem 78:3084–3089. doi:10.1021/ac0519460
13. de Mello AJ (2003) Seeing single molecules. Lab Chip 3:29N–34N
14. Whitesides G (2006) The origins and the future of microfluidics. Nature 442:368–373. doi:10.1038/nature05058
15. Neuži P, Giselbrecht S, Länge K, Huang TJ, Manz A (2012) Revisiting lab-on-a-chip technology for drug discovery. Nat Rev Drug Discov 11:620–632. doi:10.1038/nrd3799
16. Nge PN, Rogers CI, Woolley AT (2013) Advances in microfluidic materials, functions, integration, and applications. Chem Rev 113:2550–2583. doi:10.1021/cr300337x
17. Lin JH, Tseng WL (2014) Design of two and three input molecular logic gates using non-Watson-Crick base pairing-based molecular beacons. Analyst 139:1436–1441. doi:10.1039/c3an02298f
18. Xianyu Y, Wang Z, Sun J, Wang X, Jiang X (2014) Colorimetric logic gates through molecular recognition and plasmonic nanoparticles. Small 10:4833–4838. doi:10.1002/smll.201400479
19. Margulies D, Melman G, Shanzer A (2005) Fluorescein as a model molecular calculator with reset capability. Nat Mater 4:768–771. doi:10.1038/nmat1469
20. Pischel U (2007) Chemical approaches to molecular logic elements for addition and subtraction. Angew Chem Int Ed Engl 46(22):4026–4040. doi:10.1002/anie.200603990
21. Margulies D, Felder CE, Melman G, Shanzer A (2007) A molecular keypad lock: a photochemical device capable of authorizing password entries. J Am Chem Soc 129:347–354. doi:10.1021/ja065317z
22. de Ruiter G, Motiei L, Choudhury J, Oded N, van der Boom ME (2010) Electrically addressable multistate volatile memory with flip-flop and flip-flap-flop logic circuits on a solid support. Angew Chem Int Ed Engl 49:4780–4783. doi:10.1002/anie.201000785
23. Rudchenko M, Taylor S, Pallavi P, Dechkovskaia A, Khan S, Butler VP Jr, Rudchenko S, Stojanovic MN (2013) Autonomous molecular cascades for evaluation of cell surfaces. Nat Nanotechnol 8(8):580–586. doi:10.1038/nnano.2013.142
24. Kou S, Lee HN, van Noort D, Swamy KM, Kim SH, Soh JH, Lee KM, Nam SW, Yoon J, Park S (2008) Fluorescent molecular logic gates using microfluidic devices. Angew Chem Int Ed Engl 47:872–876. doi:10.1002/anie.200703813
25. Cheow LF, Yobas L, Kwong D (2007) Digital microfluidics: droplet based logic gates. Appl Phys Lett 90:054107. doi:10.1063/1.2435607
26. Toepke MW, Abhyankar VV, Beebe DJ (2007) Microfluidic logic gates and timers. Lab Chip 7:1449–1453. doi:10.1039/B708764K
27. Zhou B, Wang L, Li S, Wang X, Hui YS, Wen W (2012) Universal logic gates via liquid-electronic hybrid divider. Lab Chip 12(24):5211–5217. doi:10.1039/c2lc40840f
28. Konry T, Walt DR (2009) Intelligent medical diagnostics via molecular logic. J Am Chem Soc 131:13232–13233. doi:10.1021/ja905125b
29. Mannerstedt K, Jansson AM, Weadge J, Hindsgaul O (2010) Angew Chem Int Ed 49, 8173
30. Mannerstedt K, Jansson AM, Weadge J, Hindsgaul O (2010) Small-molecule sensing: a direct enzyme-linked immunosorbent assay for the monosaccharide Kdo. Angew Chem Int Ed Engl 49:8173–8176. doi:10.1002/anie.201003435
31. Cohen N, Sabhachandani P, Golberg A, Konry T (2015) Approaching near real-time biosensing: microfluidic microsphere based biosensor for real-time analyte detection. Biosens Bioelectron 66:454–460. doi:10.1016/j.bios.2014.11.018
32. Feldmann M, Maini RN (2003) Lasker clinical medical research award. TNF defined as a therapeutic target for rheumatoid arthritis and other autoimmune diseases. Nat Med 9:1245–1250. doi:10.1038/nm939
33. Marques LJ, Zheng L, Poulakis N, Guzman J, Costabel U (1999) Pentoxifylline inhibits TNF-alpha production from human alveolar macrophages. Am J Respir Crit Care Med 159:508–511. doi:10.1164/ajrccm.159.2.9804085
34. Locksley RM, Killeen N, Lenardo MJ (2001) The TNF and TNF receptor superfamilies: integrating mammalian biology. Cell 104:487–501. doi:10.1016/S0092-8674(01)00237-9